



Experiment Report Form

The double page inside this form is to be filled in by all users or groups of users who have had access to beam time for measurements at the ESRF.

Once completed, the report should be submitted electronically to the User Office via the User Portal:
<https://www.esrf.fr/misapps/SMISWebClient/protected/welcome.do>

Deadlines for submission of Experimental Reports

Experimental reports must be submitted within the period of 3 months after the end of the experiment.

Experiment Report supporting a new proposal (“relevant report”)

If you are submitting a proposal for a new project, or to continue a project for which you have previously been allocated beam time, you must submit a report on each of your previous measurement(s):

- even on those carried out close to the proposal submission deadline (it can be a “*preliminary report*”),
- even for experiments whose scientific area is different from the scientific area of the new proposal,
- carried out on CRG beamlines.

You must then register the report(s) as “relevant report(s)” in the new application form for beam time.

Deadlines for submitting a report supporting a new proposal

- 1st March Proposal Round - **5th March**
- 10th September Proposal Round - **13th September**

The Review Committees reserve the right to reject new proposals from groups who have not reported on the use of beam time allocated previously.

Reports on experiments relating to long term projects

Proposers awarded beam time for a long term project are required to submit an interim report at the end of each year, irrespective of the number of shifts of beam time they have used.

Published papers

All users must give proper credit to ESRF staff members and proper mention to ESRF facilities which were essential for the results described in any ensuing publication. Further, they are obliged to send to the Joint ESRF/ ILL library the complete reference and the abstract of all papers appearing in print, and resulting from the use of the ESRF.

Should you wish to make more general comments on the experiment, please note them on the User Evaluation Form, and send both the Report and the Evaluation Form to the User Office.

Instructions for preparing your Report

- fill in a separate form for each project or series of measurements.
- type your report in English.
- include the experiment number to which the report refers.
- make sure that the text, tables and figures fit into the space available.
- if your work is published or is in press, you may prefer to paste in the abstract, and add full reference details. If the abstract is in a language other than English, please include an English translation.



Measuring residual strains at the interface between photo-cured polymer dental filling materials and simulated tooth structures

Experiment number:
28-01-1282

Beamline: BM28	Date of experiment: from: 20/07/2021 to: 27/07/2021	Date of report:
Shifts: 24	Local contact(s): Dr. Laurence Bouchenoire	<i>Received at ESRF:</i>
Professor Owen Addison (King's College London) Dr. Slobodan Sirovica (Queen Mary University of London) Ms. Yilan Guo (King's College London)		

1. Abstract

Photo-activated resin-composite dental tooth fillings are routinely set using multi-diode (LEDs) light curing units, within cavities with a range of aspect ratios, generating multiple curing zones within the prosthetic which polymerise at different rates. We have previously demonstrated using in-situ synchrotron X-ray scattering that accelerating photo-polymerisation within these systems confers greater transient and residual strains which are stored within the resin polymer network structure. Our initial study characterised the dynamic behaviour of the bulk material however the impact that heterogenous photo-polymerisation, which will impact the physico-mechanical properties of the material, has on the formation and pattern of residual strain within the material is yet to be elucidated. In this study we have used synchrotron X-ray scattering to (i) spatially resolve the pattern of polymer chain segment extension for experimental resins photo-cured with a multi-LED light source and (ii) understand the formation of residual strains as a function of system constraint. Here, we demonstrate that accelerating polymerisation locally, spatially imprints different polymer conformations into the resin matrix. Additionally, greater system constraint inhibits the extension and packing of polymer chains, likely transferring residual strains to the adhered substrate.

2. Experimental details

Sample preparation: Experimental resins were formulated by combining Bis-GMA and TEGDMA monomers in 80/20, 60/40 and 40/60 (Bis-GMA/TEGDMA) wt% ratios with photo-initiator as either 0.2 wt% Camphorquinone (CQ) with 0.8 wt% of its tertiary amine N,N-dimethylaminoethyl-methacrylate (DMAEMA) or 1 wt% TPO to introduce extremes in the rate of conversion. For the first experimental objective, resins were photo-polymerised prior to the experiment within a stainless-steel ring (internal diameter =15 mm, thickness = 0.9 mm) using a commercial multi-LED inhomogeneous light curing unit (LCU) (Bluephase Style 20i, Ivoclar Vivadent, Schaan, Lichtenstein) at an intensity of 1200 mWcm⁻² for 20 s to form solid disc specimens. For the second experimental objective 60/40 wt% resins were photo-cured, using a nominally spatially homogenous LCU at an intensity of 700 mWcm⁻² for 20 s, within either Teflon or Li-ceramic washers of increasing aperture size (2,4,6,8,10 mm) to represent conditions of relatively low and high system constraint respectively.

Synchrotron X-ray scattering mapping: Synchrotron X-ray scattering measurements were performed on the XMaS (BM28) beamline at the European Synchrotron Radiation Facility (ESRF, Grenoble, France). An incident X-ray energy of 19 keV was used, equivalent to a wavelength (λ) of 0.6526 Å, with a beam size of 100 μ m \times 100 μ m (horizontal \times vertical) defined using vacuum tube slits. Resin disc samples were mounted normal to the impinging X-rays in a transmission geometry onto a travelling x-y sample stage to allow measurements in two orthogonal directions perpendicular to the X-ray beam. Measurements were carried out in air at 23 \pm 1 C° with light excluded.

Mapping measurements were conducted at 0.1 mm (horizontal and vertical) increments in the plane of the sample face. 2D X-ray scattering images were collected using a Pilatus (P3-1M) area detector (Dectris Ltd., Baden-Daettwil, Switzerland), with a 981×1043 pixel format (pixel size = $172 \times 172 \mu\text{m}^2$), placed 659 mm behind the sample to cover a q range of ~ 0.1 to 2.4 \AA^{-1} where $q = 4\pi \sin\theta/\lambda$. Scattering data were collected with a 5 s count time and a 2.7 ms readout time and a helium filled flight tube was employed to minimise air scattering. Due to the high user demand of synchrotron facilities which limits the duration of experiments combined with relatively large maps, measurements for each unique sample composition were not repeated.

The contribution of the X-ray beam to the measurements i.e. beam damage, was assessed by conducting observations for 10 min in a fixed position on a 60/40 wt% (Bis-GMA/TEGDMA) test specimen. To aid data analysis, measurements were taken for direct beam, empty sample containers and a silver behenate calibration standard. Scattering patterns were normalised to the incident monitor intensity and background corrected. Data were integrated over 360° to produce a 1D output using the pyFAI module (version 0.19.0, 2020, ESRF)(1,2) and were subsequently fitted with pseudo-Voigt profiles to determine the spatial distribution of peak positions and changes in the peak fullwidth at half maximum (FWHM) in the sample plane. The peak position(s) correspond to the measured average correlation length(s) whilst the FWHM represents the distribution of correlation lengths within the system. Chain extension was calculated by subtracting final correlation lengths from the principal correlation length of the monomer resin blend.

Results

Figure 1 shows exemplar X-ray scattering data for a 60/40 (Bis-GMA/TEGDMA) wt% pre-cured resin disc. It can be seen that two broad peak features are located at ~ 1.25 and 1.9 \AA^{-1} corresponding to real space correlation lengths of approximately 5 and 3.3 \AA . The principal scattering feature located at $\sim 1.25 \text{ \AA}^{-1}$ has previously been attributed to short-range polymer chain segment structures within the methacrylate functional groups and ethylene glycol bridges of the constituent monomers in addition to separation distances between adjacent cross-linked polymer chains(3,4). Peak positions at lower values of q for this scattering feature correspond to greater polymer chain segment extension within the aforementioned structures. The broader scattering peak at higher q values is ascribed to Van der Waals separation distances between residual monomer within the system.

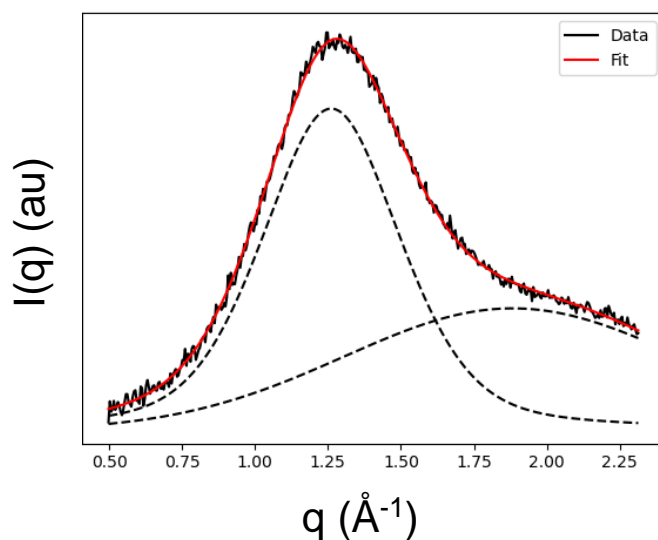


Figure 1. X-ray scattering data for a pre-cured 60/40 (Bis-GMA/TEGDMA) wt% resin disc specimen. Deconvolution of the data reveals two underlying broad peaks located at approximately ~ 1.25 and 1.9 \AA^{-1} .

Objective 1

Figure 2 illustrates spatial heterogeneity within representative 60/40 (Bis-GMA/TEGDMA) wt% resin disc specimens. Specifically, **Figure 2a** and **b** illustrate the spatial distribution of the temperature increase during photo-polymerisation in resin disc specimens, where temperature increase is a surrogate for the rate of reactive group conversion, for resins initiated with either CQ (**Figure 2a**) or TPO (**Figure 2b**) when irradiated with the multi-LED LCU (positions of respective LEDs are overlaid for clarity). It can be seen that conversion and

specifically faster conversion of the resin matrix is spatially confined to regions irradiated by LEDs with emission spectra which overlap with the absorption spectra of the photo-initiator. It can be seen in **Figures 2 c** and **d** that the pattern of polymer chain segment extension for CQ and TPO based systems respectively correspond to the location of the constituent visible blue and UV LED light sources.

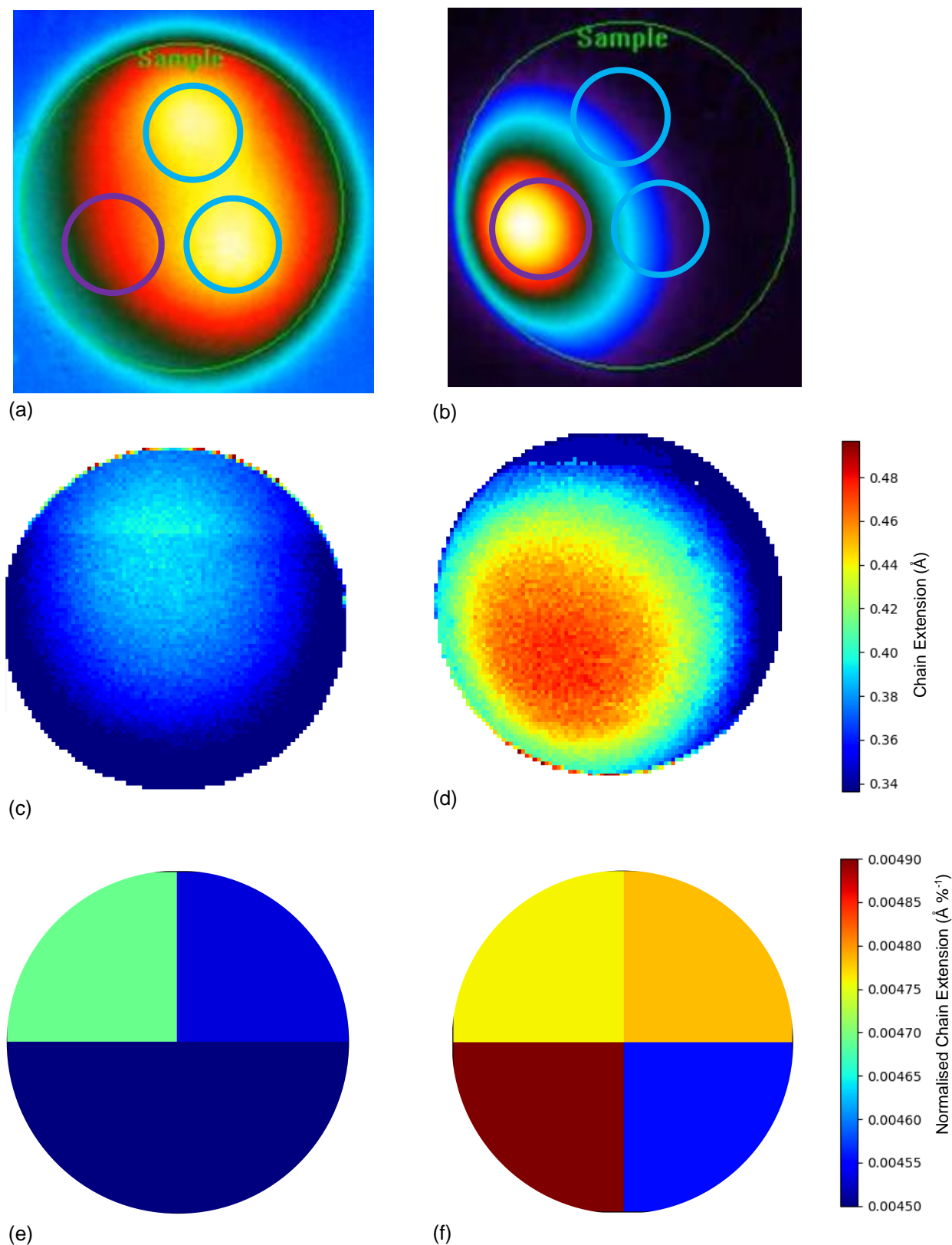


Figure 2. Top row: The spatial distribution of temperature increases within Bis-GMA/TEGDMA resin disc specimens during photo-polymerisation for systems initiated with either (a) CQ or (b) TPO photo-initiator species. The positions of the visible blue and UV LED lights are overlaid for clarity, activating primarily CQ and TPO photo-initiators respectively. Middle row: Polymer chain segment extension visualised over the same resin disc specimens for (c) CQ and (d) TPO initiated systems. Bottom row: Polymer chain segment extension normalised, within quadrants, to bulk FT-MIR ATR spectroscopy measurements of reactive group conversion within the (e) CQ and (f) TPO based resins.

However, direct correlations between X-ray data and relative differences in polymerisation rate are complicated by differences in reactive group conversion for each polymerising system. Here, chain extension has been normalised to FT-MIR ATR spectroscopy measurements of reactive conversion for each quadrant of the respective resin disc specimens (high resolution micro-spectroscopic measurements are forthcoming). Normalising the increase in correlation length with respect to reactive group conversion demonstrates that accelerating polymerisation locally, spatially imprints different polymer conformations per converted monomer.

Objective 2

Figure 3 shows the average chain extension for (a) CQ and (b) TPO based 60/40 wt% resin disc specimens as a function of system constraint i.e. cured within Teflon (lower constraint) or Li-ceramic (higher constraint), and aspect ratio which was mediated by the aperture of the washer. It can be seen that for both photo-initiator systems, chain extension is greater in the lower constraint systems and increases with the diameter of the washer aperture.

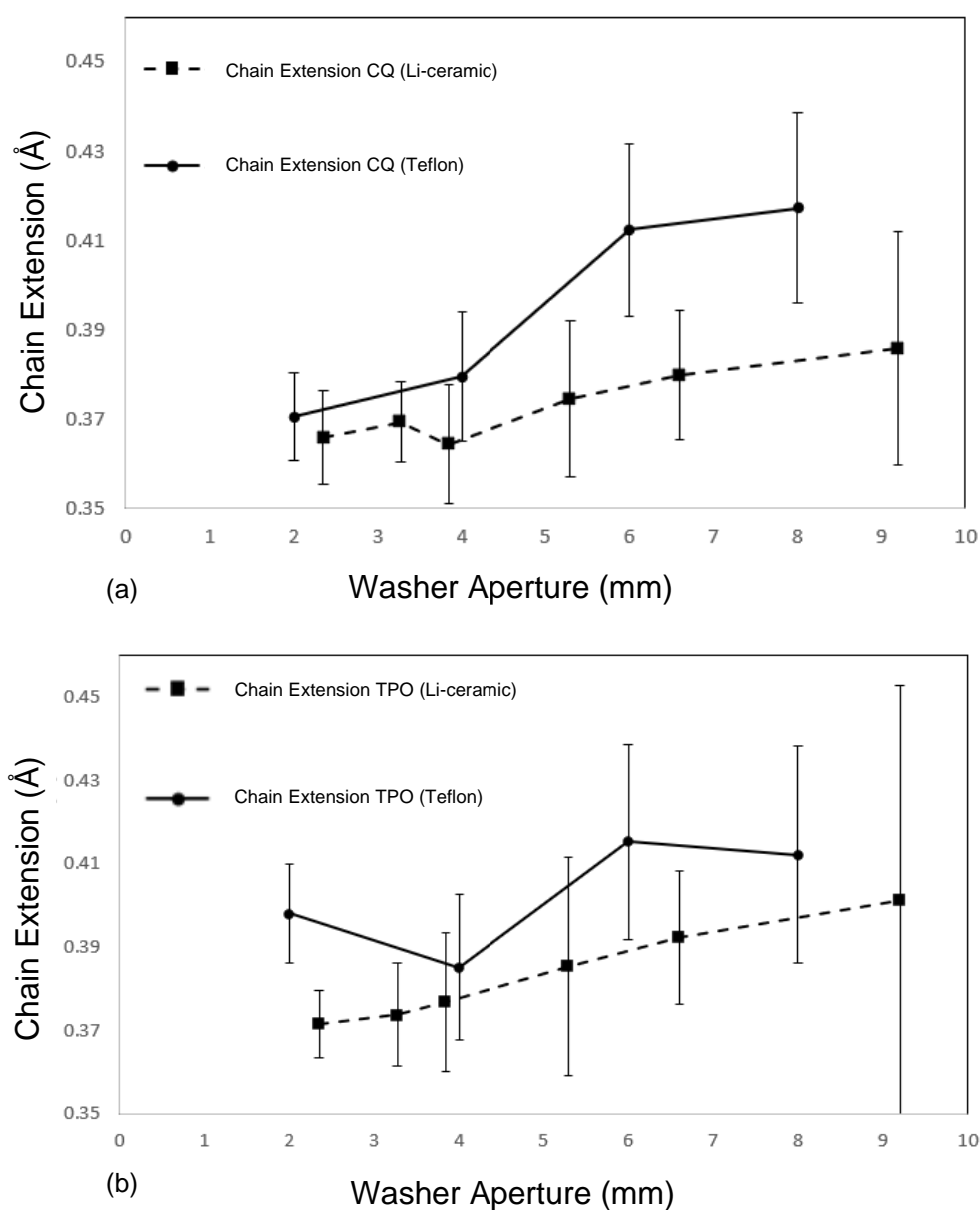


Figure 3. Polymer chain segment extension as a function of low (Teflon, solid line) or high (Li-ceramic, broken line) system constraint and aspect ratio for (a) CQ and (b) TPO initiated 60/40 (Bis-GMA/TEGDMA) wt% resin disc specimens.

Conclusions and future work

In this study we have demonstrated that using multi-LED light curing units to photo-cure experimental dental resins generates localised regions with different polymer rrrrrrrr and residual strains, corresponding to the locations of the constituent LED light sources, as a function of relative differences in polymerisation rate. Furthermore, system constraint impacts polymer chain segment extension where greater constraint likely inhibits volumetric shrinkage and the associated extension and packing of polymer chains. Similarly, as the washer aperture increases the proportion of unconstrained resin becomes larger, allowing greater chain extension. Future work will focus on conducting dynamic measurements of chain extension, specifically at the resin-substrate interface using a focussed beam, to explore the evolution of residual strains as a function of system constraint and aspect ratio.

References

1. Ashiotis, G., Deschildre, A., Nawaz, Z., Wright, J.P., Karkoulis, D., Picca, F.E., et al. The fast azimuthal integration Python library: pyFAI. *J. Appl. Crystallogr.* 2015. 24;48(Pt 2):510–9.
2. Kieffer, J., Valls, V., Blanc, N. & Hennig, C. New tools for calibrating diffraction setups. *J. Synchrotron Radiat.* 2020. 1;27: 558-566.
3. Sirovica, S., Skoda, M.W.A., Podgorski, M., Thompson, P.B.J., Palin, W., Guo, Y., et al. Structural Evidence That the Polymerization Rate Dictates Order and Intrinsic Strain Generation in Photocured Methacrylate Biomedical Polymers. *Macromolecules.* 2019. 10;52(14):5377–88.
4. Sirovica, S., Guo, Y., Guan, R., Skoda, M.W.A., Palin, W.M., Morrell, A.P., et al. Photo-polymerisation variables influence the structure and subsequent thermal response of dental resin matrices. *Dent. Mater.* 2020. 36;3:343-352.